Numerical versus analytical models of laser-induced population redistribution in Rydberg atoms

A. Wójcik and R. Parzyński
Quantum Electronics Laboratory, Institute of Physics, A. Mickiewicz University, Umultowska 85, 61-614 Poznań, Poland
(Received 6 July 1998)

Our recent approximate analytical results on the evolution of the initial state and the excitation from this state of a band of high Rydberg states by an optical pulse [Phys. Rev. A **55**, 2144 (1997)] are compared with more exact numerical results. The difference between the two approaches is that the approximations of representative atom-field couplings and equidistant spacing of high Rydberg states, applied in the analytical model, are removed in the numerical model. We find that the approximate analytical model is not able to reproduce all the results of the more exact numerical model, if the laser pulse is very short (i.e., much shorter that the Kepler period of the resonantly excited high Rydberg state) or very intense (i.e., when the Rabi period for the resonant transition is substantially shorter than the above Kepler period). This mainly concerns the redistribution of the population over different Rydberg states. The analytical model predicts a symmetric distribution centered around the resonantly excited Rydberg state, irrespective of the pulse duration and intensity, while the numerical model allows an asymmetric distribution with its maximum shifted towards lower Rydberg states. Despite the above-stated difference, the analytical model is able to give preliminary results for the total population of all the excited Rydberg states and the evolution of the initial state, imitating at least qualitatively the results of the numerical model in certain time and intensity scales. [S1050-2947(99)06301-5]

PACS number(s): 42.50.Hz, 32.80.Rm

I. INTRODUCTION

In our recent paper [1], we studied a model of the optical pulse excitation of the hydrogen atom from the circular state $|0\rangle=|n_0 l_0=n_0-1 m_0=l_0\rangle=|433\rangle=4f(m_0=3)$ to a band of high *ng* Rydberg states around $n=40$. The excited states were allowed to decay to *f* and *h* continuum states. The excitation was produced by a light pulse of linear polarization and duration not exceeding the representative Kepler period of the band of the directly excited Rydberg states. In the model, the population directly excited to the Rydberg band of the angular momentum quantum number l_0+1 (that marked by $j=1$ in Fig. 1) was allowed to migrate partially to Rydberg bands of higher angular momenta (those marked by $j=2,3,4,\ldots$) due to nonresonant degenerate Raman transitions. Under the rectangular pulse and rotating-wave assumptions, this model resulted in a compact analytical solution for the bound-state amplitudes provided that we used the so-called representative-coupling and equidistant-level (harmonic) approximations.

The approximation of representative couplings was based on the fact that for $n\gg 1$ both the one-photon and the Raman two-photon matrix elements did not change significantly if *n* was replaced by $n+1$. As a result, a set of slightly *n*-dependent matrix elements was replaced by one representative matrix element. In the calculations in question [1], the representatives for one-photon bound-bound and bound-free matrix elements were those involving the Rydberg state with $n=40$ while for two-photon Raman matrix elements they were between the Rydberg states with *n* equal to 40 and 41. It is believed that the representative-coupling approximation should work satisfactorily if only those Rydberg states which are tightly concentrated around $n=40$ are effectively populated during the process. One can, however, expect that a very short laser pulse of high intensity will disperse the population over a large number of Rydberg states not necessarily concentrated around $n=40$ [2], thus violating the idea of representative couplings. This would impose limitations on the applicability of the Laplace solution found in [1] in the framework of the representative-coupling approximation.

To transform the Laplace solution obtained to the time domain, we made in [1] one approximation more, the so-called harmonic approximation, consisting in the treatment of the Rydberg levels around $n=40$ as equidistant ones with the spacing equal to that between the levels with $n=40$ and 41 in the real hydrogen atom. This harmonic approximation has its justification in the scaling of the actual energy spacing as $1/n^3$ for $n\gg 1$, which leaves the spacing nearly unchanged when $n\rightarrow n+1$. Also this approximation should work well if

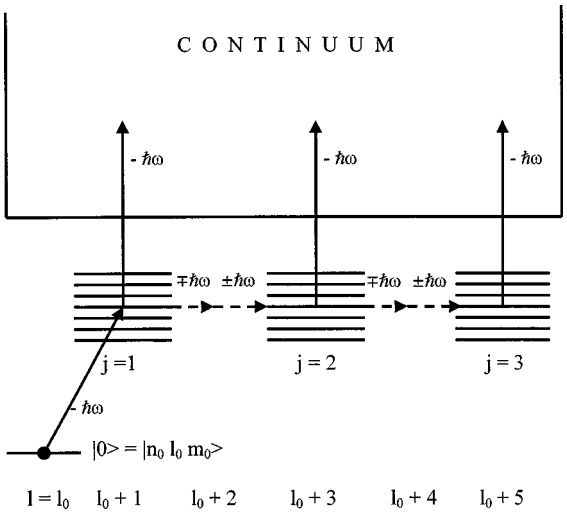

FIG. 1. A schematic representation of the excitation process extended to include the ionization losses and the nonresonant Raman migration of the population from the directly excited towards higher-*l* Rydberg states (dashed arrows). The minus (plus) sign at $\hbar\omega$ corresponds to the absorption (emission) of a photon.

the band of the excited Rydberg states is not too broad with the center at $n=40$. Applying the harmonic approximation, we analytically transformed the Laplace solution to the time domain following the prescription of Stey and Gibberd [3] originally invented to solve a different problem.

The above-described representative-coupling and harmonic approximations enabled us to find, in a purely analytical way, the Schrödinger amplitudes for the population of different bound states of the model (Fig. 1) at the end of the laser pulse. We used these analytical amplitudes to study the effect of laser intensity on the decay of the initial state $4f(m_0=3)$, the excitation of the *ng* Rydberg states, the nonresonant Raman migration of the population from the *ng* to higher-*l* Rydberg states, and the atomic ionization (see [4–8] for an analysis of relevant models along different lines). However, the question arises to what extent the results in [1] suffer from the two main approximations we made, namely, the representative-coupling and harmonic approximations. To answer this question, we shall reconsider along a numerical line the process of excitation shown in Fig. 1 without applying these two approximations.

II. LAPLACE SOLUTION WITHOUT THE REPRESENTATIVE-COUPLING AND HARMONIC APPROXIMATIONS

Let us take the set of equations (12)–(14) in [1] as the starting point in our reconsideration. It is the Laplace-transformed set ($t\rightarrow s$) for the Schrödinger population amplitudes, b, written in the rectangular-pulse and rotating-wave approximations. Leaving unchanged the notation introduced in [1], we use $\tilde{b}_0$ for the Laplace-transformed population amplitude of the initial state $|0\rangle$, $\tilde{b}_{nj}$ for the Laplace-transformed amplitude of the nth state in the jth Rydberg band of the angular momentum quantum number $l_j=l_0+(2j-1)$, δ_{nj} for the field-free detuning from resonance between the initial state and the nth state in the jth band, $\Omega_{0,n1}$ for the Rabi frequency connecting the initial state to the nth state in the first Rydberg band, and $D_{nj,n'j'}$ for the nonresonant Raman couplings between Rydberg states from the same ($j'=j$) and neighboring ($j'=j\pm1$) bands. In the energy scale with its zero ascribed to the initial-state atom plus the accompanying photons, the equations for the Laplace-transformed amplitudes are

$$\tilde{b}_0=\frac{1}{s}\left(1-i\sum_n \Omega_{0,n1}\tilde{b}_{n1}\right), \tag{1}$$

$$\tilde{b}_{n1}=\frac{-1}{s-i\delta_{n1}}\left(i\Omega_{0,n1}\tilde{b}_0+\sum_{n'} D_{n1,n'1}\tilde{b}_{n'1}+\sum_{n'} D_{n1,n'2}\tilde{b}_{n'2}\right), \tag{2}$$

$$\tilde{b}_{nj}\overset{j\geq 2}{=}\frac{-1}{s-i\delta_{nj}}\left(\sum_{n'} D_{nj,n'j}\tilde{b}_{n'j}+\sum_{n'} D_{nj,n',j-1}\tilde{b}_{n',j-1}+\sum_{n'} D_{nj,n',j+1}\tilde{b}_{n',j+1}\right). \tag{3}$$

In [1], the above set of equations was solved by applying the representative-coupling approximation, which resulted in the extraction of the matrix elements before the summation sign over n. Instead, we now apply a better approximation exploiting the fact that, for $n\gg1$, the Rabi frequency scales as $1/n^{3/2}$ while the Raman couplings scale as $1/(nn')^{3/2}$ [9,10]. In other words, we factorize the one- and two-photon couplings as

$$\Omega_{0,n1}=\Omega/n^{3/2},$$

$$D_{nj,n'j'}=D_{jj'}/(nn')^{3/2}, \tag{4}$$

with Ω and $D_{jj'}$ being n-independent parameters. There is no problem with calculating $\Omega_{0,n1}$ [10], but much effort is needed to find $D_{nj,n'j'}$ in the second-order perturbation theory. In [1], we gave a rough estimation of the real part of the two-photon Raman matrix element between a pair of high Rydberg states, based on the expansion of this element in the inverse powers of photon energy. For the assumed photon energy (resonant to the $n_0=4\rightarrow n=40$ transition), this expansion is believed to work satisfactorily for the majority of discrete intermediate states as well as those continuum intermediate states whose energy is much smaller than the photon energy. With only these intermediate states included, and the atom-field interaction Hamiltonian taken in the velocity rather than the length form, we found that already the first term of the expansion mentioned results in a nontrivial expression for the Raman matrix element [Eq. (10) in [1]]. In the diagonal case ($n=n'$, $j=j'$), this expression gives the shift of high Rydberg states scaled as n^{-3} [Eq. (11) in [1]]. This scaling factor agrees with the one obtained by Fedorov and Movsesian [11] along a different line based on the semiclassical approximation of dipole matrix elements. Because Fedorov and Movsesian used the length form of the atom-field interaction Hamiltonian, their semiclassical result emerged from the second term of the expansion of the two-photon matrix element in the inverse powers of photon energy.

We insert the factorization ansatz (4) into Eqs. (1)–(3), then divide Eqs. (2) and (3) by $n^{3/2}$, and finally sum the latter ones over all Rydberg states in a given j band, obtaining

$$\tilde{b}_0=\frac{1}{s}(1-i\Omega K_1), \tag{5}$$

$$(1+P_1D_{11})K_1=-P_1(i\Omega\tilde{b}_0+D_{12}K_2), \tag{6}$$

$$(1+P_jD_{jj})K_j\overset{j\geq 2}{=}-P_j(D_{j,j-1}K_{j-1}+D_{j,j+1}K_{j+1}), \tag{7}$$

where

$$K_j=\sum_n \tilde{b}_{nj}/n^{3/2} \tag{8}$$

and

$$P_j=\sum_n \frac{1}{n^3(s-i\delta_{nj})}. \tag{9}$$

The point is that Eqs. (5)–(7), obtained with the use of the factorization ansatz (4), have the same structure as the appropriate equations derived previously in the representative-coupling approximation [Eqs. (15), (19), and (20) in [1]]. However, there are essential differences in the definitions of K_j and P_j [Eqs. (8) and (9)]. As compared to [1], the present K_j and P_j include the extra powers of n in the summands. It will be shown soon that the new P_j introduces serious difficulties when one wants to transform the solution from the Laplace s domain to the time t domain. In the Laplace domain, the solutions to Eqs. (5)–(7) and then those to Eqs. (2) and (3) are found straightforwardly following the line of our previous paper [1]. The result is

$$\tilde{b}_0=\frac{1}{s+\Omega^2 P_1 G_1}, \tag{10}$$

$$\tilde{b}_{nj}=\frac{1}{n^{3/2}(s-i\delta_{nj})}\frac{K_j}{P_j}, \tag{11}$$

where

$$K_j=i(-1)^j\Omega\left(\prod_{k=1}^{j-1} D_{k,k+1}\right)\left(\prod_{k=1}^{j} P_k G_k\right)\tilde{b}_0, \tag{12}$$

with G_j being the continued fraction

$$G_j=\frac{1}{1+P_j D_{jj}[1-(D_{j,j+1}^2/D_{jj})P_{j+1}G_{j+1}]}, \tag{13}$$

fulfilling the boundary condition

$$G_N=\frac{1}{1+P_N D_{NN}}. \tag{14}$$

Here $N=j_{\max}$ numbers the last Rydberg band in the chain of nonresonant Raman couplings, i.e., the band with $l_N=l_0+(2N-1)$. For $N=1$, the first product over k in Eq. (12) for K_j should be read as 1.

In the representative-coupling approximation, P_j was free of the factor n^3 in the denominator of the summand in Eq. (9). Moreover, applying in [1] the harmonic approximation for the spacing between high Rydberg states, we replaced P_j by a coth function having the Laplace variable s in its argument. These two approximations made the transformation of the Laplace solution to the short-time domain (the pulse duration shorter than the Kepler period of the resonantly excited Rydberg state) free of trouble. With neither the representative-coupling nor harmonic approximations, we now use P_j in the exact form of Eq. (9) with the detuning $\delta_{nj}=\delta_n=\omega-(n_0^{-2}-n^{-2})\omega_{\rm at}/2$, where ω stands for the laser-radiation frequency while $\omega_{\rm at}=4.13\times10^{16}\ {\rm s}^{-1}$ for the atomic unit of frequency. With the above detuning, typical of the hydrogenic energy structure, P_j of Eq. (9) can be represented [12,13] in terms of the $\Psi(x)$ digamma function [14], i.e., the logarithmic derivative of the Euler gamma function:

$$\psi(x)=\psi(1)-\frac{1}{x}+x\sum_{n=1}^{\infty}\frac{1}{n(n+x)}, \tag{15}$$

where $-\psi(1)=0.5772\ldots$ is the Euler constant. In terms of a new variable

$$c=\frac{1}{2}\left(\frac{is}{\omega_{\rm at}}+\frac{\omega}{\omega_{\rm at}}-\frac{1}{2n_0^2}\right)^{-1}, \tag{16}$$

P_j of Eq. (9) looks like

$$\begin{aligned} i\omega_{\rm at}P_j&=-2c\sum_{n=\bar{n}}^{\infty}\frac{1}{n(n^2+c)}\\ &=-\sum_{n=\bar{n}}^{\infty}\frac{1}{n}\left(\frac{i\sqrt{c}}{n+i\sqrt{c}}+\frac{-i\sqrt{c}}{n-i\sqrt{c}}\right)\\ &=2\left(\psi(1)+c\sum_{n=1}^{\bar{n}-1}\frac{1}{n(n^2+c)}\right)\\ &\quad-[\psi(i\sqrt{c})+\psi(-i\sqrt{c})]\\ &=f(c), \end{aligned} \tag{17}$$

while its first derivative with respect to the Laplace variable, to be required later on, looks like

$$\begin{aligned} \frac{dP_j}{ds}&=\left(\frac{2c}{\omega_{\rm at}}\right)^2\sum_{n=\bar{n}}^{\infty}\frac{n}{(n^2+c)^2}\\ &=\left(\frac{2c}{\omega_{\rm at}}\right)^2\frac{i}{4\sqrt{c}}\sum_{n=\bar{n}}^{\infty}\left(\frac{1}{(n+i\sqrt{c})^2}-\frac{1}{(n-i\sqrt{c})^2}\right)\\ &=\left(\frac{2c}{\omega_{\rm at}}\right)^2\left(\frac{i}{4\sqrt{c}}[\psi'(i\sqrt{c})-\psi'(-i\sqrt{c})]\right.\\ &\quad\left.-\sum_{n=1}^{\bar{n}-1}\frac{n}{(n^2+c)^2}\right), \end{aligned} \tag{18}$$

where

$$\psi'(x)=\frac{d\psi(x)}{dx}=\sum_{n=0}^{\infty}\frac{1}{(n+x)^2} \tag{19}$$

is the trigamma function [14]. In Eqs. (17) and (18), $\bar{n}$ must be taken substantially greater than n_0 for the condition of the rotating-wave approximation to be well satisfied.

III. APPLICATION TO THE $4f(m_0=3)$ INITIAL-STATE CASE

Generally, it is not possible to neglect the nonresonant Raman transitions from the directly excited Rydberg band of $l_1=l_0+1$ to higher-l Rydberg bands [15,16]. However, our preliminary results [1], obtained with the use of both the representative-coupling and harmonic approximations, suggest that when the $ng(m=3)$ Rydberg states around $n=40$ are one-photon excited from the initial circular state $4f(m_0=3)$, then such nonresonant Raman transitions to higher-l Rydberg states are inefficient in the laser intensity range of our consideration. Focusing on this case, we set $N=j_{\max}=j=1$ in Eqs. (10)–(14), obtaining $G_1=(1+P_1D_{11})^{-1}$ and $K_1/P_1=-i\Omega G_1\tilde{b}_0$. With these simplified versions of G_1

and K_1/P_1, we transform the Laplace solutions for $\tilde{b}_0$ and $\tilde{b}_{n1}$ [Eqs. (10 and (11)] to the time domain applying the method of the elementary fraction decomposition. This method requires that the roots s_k $(k=1,2,3,\ldots)$ of the algebraic equation $s+\Omega^2 P_1 G_1=0$ be found. In the alternative c-variable language [see Eq. (16)], the last equation reads

$$f(c)=\left(i\,\frac{D_{11}}{\omega_{\rm at}}-\frac{2(\Omega/\omega_{\rm at})^2}{\dfrac{1}{c}-\dfrac{2\omega}{\omega_{\rm at}}+\dfrac{1}{n_0^2}}\right)^{-1}, \tag{20}$$

with $f(c)$ given by Eq. (17). Writing $c=x+iy$, Eq. (20) can be split into its real and imaginary parts giving a pair of coupled equations for two real variables x and y. For a fixed ω and n_0, this set can be solved numerically for different intensities applying, e.g., the secant method. Having known the solutions $c_k=x_k+iy_k$ for a given intensity and, thus, s_k from Eq. (16), we decompose Eqs. (10) and (11) as

$$\tilde{b}_0=\sum_k \frac{R_k}{s-s_k}, \tag{21}$$

$$\tilde{b}_{n1}=\tilde{b}_n=-\frac{i\Omega}{n^{3/2}}\frac{1}{s-i\delta_n}\sum_k \frac{R_k G_1(s_k)}{s-s_k}, \tag{22}$$

where

$$R_k=\frac{1}{1+\Omega^2\left(G_1^2\dfrac{dP_1}{ds}\right)_k}, \tag{23}$$

and $(\cdots)_k$ means the value of $(\cdots)$ at $s=s_k$. When Laplace inverted, Eqs. (21) and (22) result in the following time-dependent Schrödinger population amplitudes of the initial $4f(m_0=3)$ and high-Rydberg $ng(m=3)$ states:

$$b_0=\sum_k R_k e^{s_k t}, \tag{24}$$

$$b_{n1}=b_n=-e^{i\delta_n t}\frac{\Omega}{n^{3/2}}\sum_k R_k G_1(s_k) f_k(t), \tag{25}$$

where

$$f_k(t)=\frac{1-e^{-i(\delta_n+is_k)t}}{\delta_n+is_k}. \tag{26}$$

IV. RESULTS

When solving numerically Eq. (20), the light was assumed to be characterized by linear polarization, and frequency resonant to the transition from the initial circular state of $n_0=4$ to the state of $n=n_r=40$ [$\omega/\omega_{\rm at}=(n_0^{-2}-n_r^{-2})/2$, $is/\omega_{\rm at}=(c^{-1}+n_r^{-2})/2$ and $\delta_n/\omega_{\rm at}=(n^{-2}-n_r^{-2})/2$]. To initiate the iteration procedure of the secant method, we had to know approximate solutions of Eq. (20) for a fixed intensity. Such approximate solutions could be found by considering, e.g., the low-intensity limit, in which the right-hand side of Eq. (20) tends to infinity. These low-intensity solutions were then used as the initial conditions when finding solutions for slightly different intensities. For a given intensity, the problem was in finding the solutions $c_k=x_k+iy_k$ of Eq. (20) contributing predominantly to the process and in evaluating the minimum number of the leading solutions. The leading solutions c_k were recognized as those producing the greatest residue R_k determined by Eq. (23). On the other hand, the minimum number of the leading solutions was estimated as the number which ensured that the condition $|\Sigma_k R_k|^2=1$ would be fulfilled to a good approximation. The last equality simply results from Eq. (24) after realizing the initial condition of the process, namely, that at $t=0$ all the population resides in the $|0\rangle=4f(m_0=3)$ state. Up to the highest intensity under our considerations (10^{12} W/cm^2), no more than about a hundred solutions c_k were sufficient for a given intensity. Having found the solutions c_k for a given intensity, we calculated for this intensity and a fixed pulse duration the population probabilities of the initial state and high Rydberg states using Eq. (24) and Eq. (25), respectively. The results obtained in this numerical way are given in Fig. 2 and as dots in Figs. 3–5.

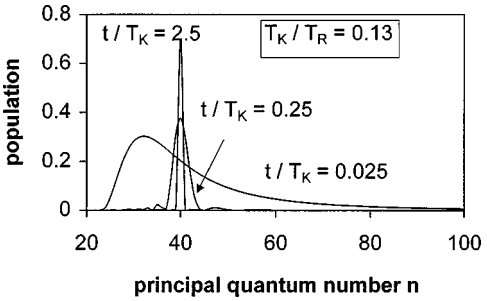

FIG. 2. The distribution of the population over Rydberg states given by the numerical model, for low-intensity pulse (7.8×10^8 W/cm^2, $T_K/T_R=0.13$) of different scaled duration t/T_K. The distributions for $t/T_K=0.25$ and 0.025 are multiplied by the factors 15 and 500, respectively.

Let us start with the analysis of the results of the numerical model (no representative-coupling and harmonic approximations made) for low intensities. By low we mean the intensities for which the Rabi frequency $\Omega_{4f,40g}$ for the resonant $4f\rightarrow 40g$ transition is smaller than the distance Δ of the $40g$ level from the nearest neighbor. In the time scale, the Rabi period for the transition, $T_R=2\pi/\Omega_{4f,40g}$, is thus longer than the Kepler period $T_K=2\pi/\Delta=9.73$ ps of the resonantly excited $n_r=40$ state. For the low intensity of 7.8×10^8 W/cm^2, for which $T_K/T_R=0.13$, we show in Fig. 2 the effect of the scaled pulse duration t/T_K on the redistribution of the population among Rydberg states differing in the principal quantum number n. As it should have been expected, only the resonant level of $n=n_r=40$ is populated if the pulse duration is longer than the Kepler period ($t/T_K=2.5$). In the opposite case of short pulse ($t/T_K=0.25$), i.e., when the Fourier bandwidth of the pulse exceeds the distance Δ between the resonant level and the nearest neighbors, the neighbors are populated as well ($n=38$–43). Further shortening of the pulse ($t/T_K=0.025$) results in the flattening and asymmetrization of the distribution and, interestingly, in the shift of the maximum of the distribution towards lower-n states ($n=32$). This shift is the resultant effect of different n dependences of the dipole matrix elements and

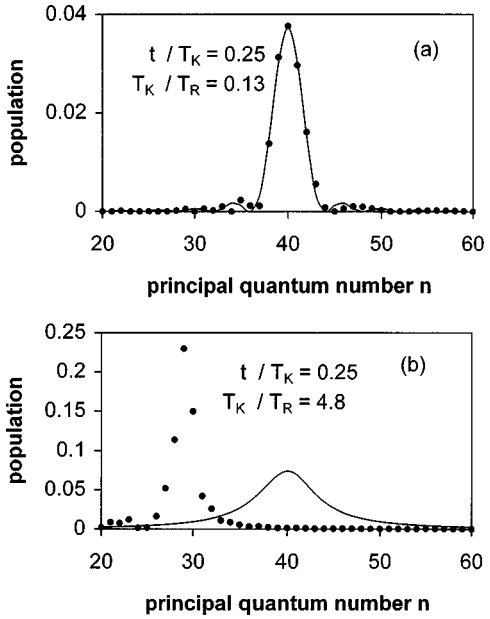

FIG. 3. The numerically (dots) and analytically (full line) calculated Rydberg-state distributions, for the pulse of duration $t/T_K=0.25$ and two different intensities [7.8×10^{10} W/cm^2 ($T_K/T_R=0.13$) and 10^{12} W/cm^2 ($T_K/T_R=4.8$)].

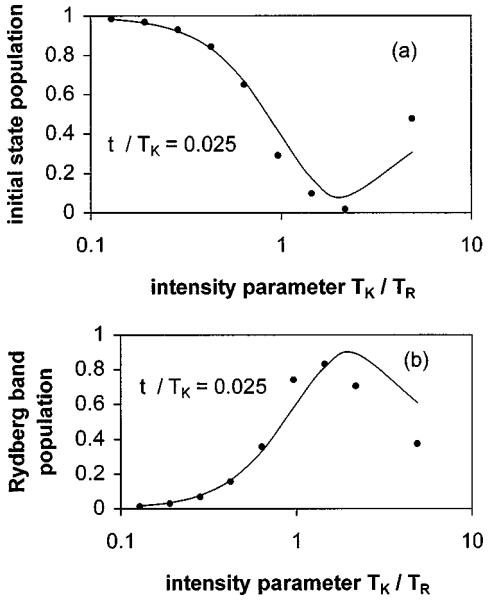

FIG. 5. The numerically (dots) and analytically (full line) calculated populations of the initial state (a) and all the excited Rydberg states (b) versus the intensity parameter T_K/T_R, for the short pulse of duration $t/T_K=0.025$.

detunings and is in conformity with the observation of Piraux *et al.* [2] made for a different physical situation. Our parameters $t/T_K=2.5$, 0.25, and 0.025 were intentionally chosen to correspond to the parameters $\rho=10^5$, 10^4, and 10^3 in Fig. 2 of the paper [2].

The shift of the maximum of the Rydberg-state distribution is what generally distinguishes the present results of the numerical model from the analytical results, i.e., those obtained by applying both the representative coupling and harmonic approximations. The analytical calculations always result in the symmetric distribution centered around $n=40$, irrespective of the intensity and duration of the optical pulse. Thus, Fig. 2 suggests that, in the low-intensity limit ($T_K/T_R=0.13$), one can expect an agreement between the analytical and numerical distributions for longer pulses. This suggestion is confirmed in Fig. 3(a) made for $t/T_K=0.25$, i.e., the pulse duration still shorter than the Kepler period. In this figure, as in all further figures, the numerical results are representend by dots while the analytical results by full lines. Figure 3(b) shows, however, that for this longer pulse ($t/T_K=0.25$) the numerical and analytical distributions cease to cover if the intensity is too high (10^{12} W/cm^2, $T_K/T_R=4.8$). Because of the high intensity, the numerical distribution is shifted to lower n and centered around $n=29$, while the analytical distribution still remains built up around $n=40$. The general conclusion that can be drawn from Fig. 2 and 3 is that if the laser pulse is too short ($t/T_K\ll1$) or/and too intense ($T_K/T_R\gg1$), the numerical redistribution of the population among different Rydberg states cannot be reproduced by the analytical redistribution.

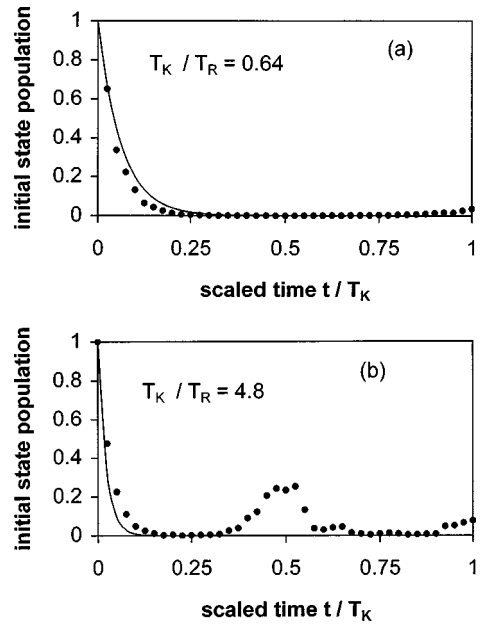

FIG. 4. The numerically (dots) and analytically (full line) calculated time dependences of the initial-state population, for two different pulse intensities [2×10^{10} W/cm^2 ($T_K/T_R=0.64$) and 10^{12} W/cm^2 ($T_K/T_R=4.8$)].

Now, let us concentrate on the time evolution of the initial-state population, $|b_0|^2$. According to [1], the analytical evolution obtained with the use of the representative-coupling and harmonic approximations results in the exponential decay up to the time equal to the Kepler period of the resonantly excited $n=40$ Rydberg state ($0\leqslant t/T_K\leqslant1$), irrespective of the pulse intensity. In Fig. 4, we compare the numerically obtained evolution implied by Eq. (24) (dots) with the analytical evolution (full line), for two strongly differing intensities: 2×10^{10} W/cm^2 ($T_K/T_R=0.64$) and 10^{12} W/cm^2 ($T_K/T_R=4.8$). For the lower intensity [Fig. 4(a)], the analytical evolution is seen to imitate pretty well the numerical evolution in the time interval considered ($t/T_K\leqslant1$). We cannot make the comparison for longer pulses because we do not know the analytical solution for b_0

in the time interval of $t/T_K > 1$. The lower intensity taken is the limit above which we observed increasing discrepancies between the analytical and numerical evolutions. These discrepancies are well pronouced in Fig. 4(b) obtained for the highest intensity considered (10^{12} W/cm^2). The numerical evolution is seen to depart profoundly from the analytical one starting from $t/T_K = 0.33$. After crossing this point the curve of the numerical evolution revives and reaches maximum at $t/T_K = 0.5$, while the curve of the analytical evolution tends monotonically to zero. The other revival of the numerical-evolution curve is observed around $t/T_K = 1$. These revivals mean that, at the highest intensity considered, the numerical solution contrary to the analytical solution allows the population to oscillate between the initial state and the band of high Rydberg states in the time scale of $0.33 < t/T_K \leqslant 1$. The apparent good reproduction of the numerical evolution by the analytical one up to $t/T_K = 0.33$ can to some extent be correlated with effective shortening of the Kepler period due to the shift of the maximum of the Rydberg-state population towards lower-n states. As seen from Fig. 3(b), made for the same intensity as Fig. 4(b), the maximum of the distribution appears for the $n = 29$ state whose Kepler period is equal to 0.38 times the Kepler period of the $n = 40$ state $[t/T_K(40) = 0.38 t/T_K(29)]$.

Figure 4 suggests that the analytical calculations performed with both the representative coupling and harmonic approximations should give the initial-state population close to the numerically calculated population in a wide intensity range, provided that the pulse duration is very short, i.e., $t/T_K \ll 1$. This suggestion is confirmed in Fig. 5(a), where it is assumed $t/T_K = 0.025$. The limited number of dots in this figure is the result of difficulties we encountered solving numerically Eq. (20), particularly for higher intensities $(T_K/T_R \geqslant 1)$. On the basis of the analysis concerning Figs. 2 and 3, we could expect that, for such a short pulse $(t/T_K = 0.025)$, the dependence of the total population of all the excited Rydberg states on laser intensity calculated within the representative-coupling and harmonic approximations should differ substantially from that calculated without them. Surprisingly, no such drastic differences are seen in Fig. 5(b); what is more, even a quantitative agreement between analytical and numerical results is obtained for low intensities $(T_K/T_R < 1)$. For higher intensities $(T_K/T_R \geqslant 1)$, there is, however, qualitative agreement only. Thus, the conclusion is that though the analytical and numerical approaches give, for short or/and intense pulses, different distributions of the population over high Rydberg states, the total Rydberg-state population suffers less from the representative-coupling and harmonic approximations.

V. SUMMARY

A comparison was made between the predictions of two models of the laser-induced redistribution of the population in Rydberg atoms. One model had the advantage of being analytical thanks to the representative-coupling and harmonic approximations [1], while the other model is numerical and does not suffer from the two approximations mentioned. It was shown that the results of the analytical model match those of the more accurate numerical model but only in some intervals of time and intensity. Two important discrepancies were found between the predictions of these models. One discrepancy concerns the population in individual excited Rydberg states in the limit of very short $(t_K/T_R \ll 1)$ or very intense $(T_K/T_R \gg 1)$ laser pulses. In these limits, the analytical model does not see the effect which results from the numerical model, namely, that of the shift of the maximum population towards a lower Rydberg state not reached resonantly from the initial state. The other discrepancy concerns the evolution of the initial state under the action of very intense pulses $(T_K/T_R \gg 1)$. In the time scale not exceeding the Kepler period of the resonantly excited Rydberg state $(t/T_K \leqslant 1)$, the analytical model results in a monotonic decay of the initial state, while the numerical model allows substantial revival of the initial-state population after complete collapse. On the other hand, it was found that, contrary to the population in the individual Rydberg states, the total population of all Rydberg states is less sensitive to the two approximations of the analytical model even in the limit of very short and very intense pulses. Moreover, for very short pulses, the analytical model give results quite well imitating those of the numerical model as far as the dependence of the initial-state population on laser intensity is concerned. To sum up, the analytical model with its representative-coupling and harmonic approximations can serve as a tool for obtaining preliminary results of qualitative character in general, not pretending to numerical accuracy. When changing the initial condition, i.e., by putting the initial population into a high Rydberg state, the model of excitation discussed in the present paper becomes similar to the previous models used in the study of interference stabilization of Rydberg atoms under the condition of resonance with some lower-lying state [17]. Numerical analysis like that in the present paper is planned for the models from [17].

ACKNOWLEDGMENTS

This work was made possible thanks to the support from the Polish Committee for Scientific Research under Grant No. 2 PO3B 078 12.

[1] A. Wójcik, R. Parzyński, and A. Grudka, Phys. Rev. A **55**, 2144 (1997).

[2] B. Piraux, E. Huens, and P. L. Knight, Phys. Rev. A **44**, 721 (1991).

[3] G. C. Stey and W. Gibberd, Physica (Amsterdam) **60**, 1 (1972).

[4] *Super-Intense Laser-Atom Physics IV*, Vol. 13 of *NATO Advanced Study Institute Series 3: High Technology*, edited by H. G. Muller and M. V. Fedorov (Kluwer Academic Publishers, Dordrecht, 1996), see references therein.

[5] Q. Su, J. H. Eberly, and J. Javanainen, Phys. Rev. Lett. **64**, 862 (1990).

[6] E. Huens and B. Piraux, Phys. Rev. A **47**, 1568 (1993).
[7] F. H. M. Faisal and L. Dimou, Acta Phys. Pol. A **86**, 201 (1994).
[8] M. Yu Ivanov, Phys. Rev. A **49**, 1165 (1994).
[9] M. S. Adams, M. V. Fedorov, V. P. Krainov, and D. D. Meyerhofer, Phys. Rev. A **52**, 125 (1995).
[10] G. Feldman, T. Fulton, and B. R. Judd, Phys. Rev. A **51**, 2762 (1995).
[11] M. V. Fedorov and A. M. Movsesian, J. Opt. Soc. Am. B **6**, 1504 (1989).
[12] A. Raczyński and J. Zaremba, J. Phys. B **19**, 3895 (1986).
[13] A. Wójcik and R. Parzyński, Phys. Lett. A **160**, 378 (1991).
[14] *Handbook of Mathematical Functions*, edited by M. Abramowitz and I. A. Stegun, NBS Series No. 55 (U.S. GPO, Washington, D.C., 1964).
[15] M. V. Fedorov, M. M. Tehranchi, and S. M. Fedorov, J. Phys. B **29**, 2907 (1996).
[16] R. Parzyński and A. Wójcik, Laser Phys. **7**, 551 (1997).
[17] M. V. Fedorov and N. P. Poluektov, Laser Phys. **7**, 299 (1997); Optics Express **2**, 51 (1998) (http://epubs.osa.org/opticsexpress); A. Wójcik and R. Parzyński, Phys. Rev. A **50**, 2475 (1994).